DALTON
FULL PAPER

Elucidation of the mechanism of carboxy ester cleavage promoted by a Cu(II) alkoxide complex of a tripodal ligand (N_3OX)

Jiang Xia,[a] Shu-an Li,[a] Yan-bo Shi,[a] Kai-bei Yu[b] and Wen-xia Tang *[a]

[a] *State Key Laboratory of Coordination Chemistry, Nanjing University, Nanjing, 210093, P.R. China*
[b] *Analysis Center, Chengdu Branch of Chinese Academy of Sciences, Chengdu, 610041, P.R. China*

Received 3rd January 2001, Accepted 17th May 2001
First published as an Advance Article on the web 21st June 2001

A solution complexation study by potentiometric titration of the new Cu(II) complexes of the tripodal ligand 2-[bis(2-aminoethyl)amino]ethanol (L) has revealed that with coordination to Cu(II), the hydroxyl group of L exhibits a rather low pK_a value of 8.5 to give Cu(II) alkoxide, which is also confirmed by solution ES-MS. Release of the second hydrogen atom from the coordinated water occurs at pK_a = 10.6 at 25 °C. X-Ray diffraction analysis of $[CuL(Cl)](ClO_4)$ revealed that Cu(II) adopts a trigonal-bipyramidal geometry, different from all the previously reported N_3OX–copper complexes. The CuL-promoted hydrolysis of 4-nitrophenyl acetate (NA) showed a second-order rate constant of 0.043 M^{-1} s^{-1} and further study of the hydrolysis mechanism provided evidence for the preference of a trans-esterification rather than a hydrolysis path. Additionally, an *ab initio* Hartree–Fock study strongly suggested that the Cu(II) alkoxide will be generated prior to Cu(II) hydroxide due to the energy preference for the former, with the energy difference estimated to be 55.77 kJ mol^{-1}, so the Cu(II) coordinated alcohol will exhibit a lower pK_a than Cu(II) coordinated water. Mulliken population analysis showed that the HOMO oxygen lone pair energy for Cu(II) alkoxide is 0.148 eV higher than that of Cu(II) hydroxide, according to which the oxygen of Cu(II) alkoxide is expected to be more nucleophilic.

Introduction

Recently, a great deal of interest has been shown in the development of artificial hydrolytic metalloenzymes.[1–7] A majority of the efforts has been focused on finding more efficient hydrolytic catalysts and elucidation of the role of metal hydroxide species in ester hydrolysis. On the other hand, the role of the metal ions in the activation of proximate alcoholic OH groups is well documented in natural metalloenzymes. One example is alkaline phosphatase, in which the Zn(II)-activated serine(102) is deprotonated and serves as an initial nucleophile to attack the phosphate and yield a phosphoseryl–enzyme intermediate which is then attacked again by the adjacent Zn(II)-bound hydroxide to recycle the hydrolysis.[8,9] A metal alkoxide group may also play an important role in the *Tetrahymena* ribozyme catalyzed transesterification of RNA.[10]

Only a few previous examples of Zn(II) alkoxide promoted ester hydrolysis have been provided by Kimura [11,12] and others,[13] who established that the Zn(II) alkoxide is a more efficient nucleophilic species than Zn(II) hydroxide. In the systematic modeling studies conducted by Kimura and co-workers, Zn(II) complexes with macrocyclic polyamines with a pendant ethoxy group (III and IV, see Scheme 1) were used, and the reactivities of the hydroxide and alkoxide species were compared in the hydrolysis of 4-nitrophenyl acetate.[11,12] In previous work, we utilized a new Zn(II)–tripodal polyamine bearing an ethoxy-podand to mimic the Zn(II)–serine in Zn(II)–serine enzymes, and found that Zn(II)–tripodal polyamine can also be a good model for hydrolytic enzymes.[14] In an elegant study, Chin *et al.* compared the reactivities and mechanisms of Cu(II) hydroxide and Cu(II) alkoxides for cleaving bis(2,4-dinitrophenyl)phosphate (BDNPP) using complexes V, VI and VII (Scheme 1), and discovered an interesting phenomenon in that the copper complex VII cleaves the phosphate diester by transesterification while the complexes V and VI cleave *via* a hydrolysis pathway.

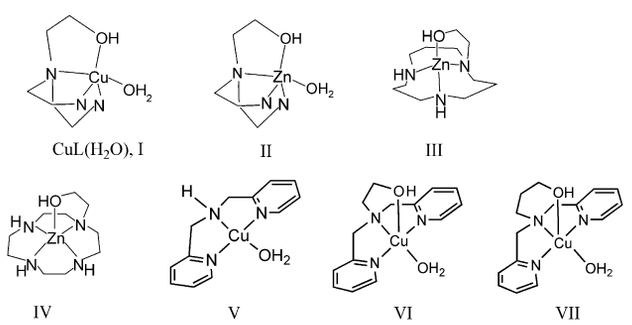

Scheme 1

The Cu(II) alkoxide promoted transesterification path is found to be two orders of magnitude faster than the hydrolysis path, *i.e.* the metal hydroxide path.[15]

To further elucidate the role of metal alkoxide in the process of ester hydrolysis, herein we report the crystal structure of the copper(II) monoperchlorate complex $\{[CuL(Cl)](ClO_4)\}$, and investigate its complexation behavior in solution. Furthermore, a study of the CuL-promoted hydrolysis of a carboxy ester, 4-nitrophenyl acetate (NA), will be reported. A detailed study of the mechanism, including *ab initio* Hartree–Fock calculations is used to provide evidence for the preference of the transesterification path over the hydrolysis path.

Experimental

Materials

2-[Bis(2-aminoethyl)amino]ethanol, (L), was synthesized as described previously.[17] The other reagents were of analytical grade from commercial sources and were used without any further purification.

[CuL(Cl)](ClO$_4$)

0.16 g (1.1 mmol) of L was dissolved in water (1 mL), to which $CuCl_2 \cdot 6H_2O$ 0.19 g (1.1 mmol) was added with stirring. Then, saturated $NaClO_4$ solution (1 mL) was added to give a clear blue solution. Blue prisms were obtained one week later by slow evaporation of the solvent. Anal. calc. for $C_6H_{17}N_3O_5Cl_2Cu$: C, 20.8; H, 4.9; N, 12.1. Found: C, 21.2; H, 4.9; N, 11.9%.

CAUTION: perchlorate salts of compounds containing organic ligands are potentially explosive, especially when heated or bumped. Only small quantities of these compounds should be prepared and handled behind suitable protective shields.

Potentiometry

Potentiometric studies were conducted with an Orion 91-04 glass combination pH electrode and an Orion microprocessor ionalyzer/901 at 25 °C. All solutions were carefully protected from air by a stream of humidified nitrogen. Standard NaOH (CO_2 free) was added *via* a spiral micro-injector. $Cu(SO_4)_2$ solution was calibrated using standardised EDTA. Double-distilled water was used throughout. The temperature of the cell was controlled by a thermostat. The system was calibrated with dilute standardised acid and alkali solution. K_w was assumed to be 13.69 at 25 °C. 0.1 M NaCl was used to adjust the ionic strength to 0.1 M. Solutions containing 1 mmol of L with or without equimolar $Cu(SO_4)_2$ were titrated to pH > 11. The complexation and protonation constants were calculated using the program BEST.[18] All data represent the average of at least two independent experiments and all the σ fit values have been reduced to less than 0.05 after optimization.

Kinetic studies

4-Nitrophenyl acetate (NA) hydrolysis was carried out by a UV-Vis method using a Shimadzu UV-240 spectrophotometer with a thermostat to control the temperature (±0.5 °C). The NA solution was added *via* a 100 μL micro-injector. The hydrolysis of NA (1.0–2.0 mM) was followed at $I = 0.10$ M (90 mM $NaNO_3$) and pH 8.09, 8.55 and 8.9 (20 mM Tris·HCl buffers) in 10% (v/v) CH_3CN aqueous solution containing [CuL(Cl)]-(ClO$_4$) (0.4–2.0 mM), by the release of 4-nitrophenolate (NP), the absorbance being measured at 400 nm. The data were processed using the initial slope procedure. Experiments were conducted at least twice.

Single-crystal X-ray crystallographic study of [CuL(Cl)](ClO$_4$)

Intensity data for the crystals of [CuL(Cl)](ClO$_4$) were collected on a Siemens P4 four-circle diffractometer with monochromated Mo-Kα ($\lambda = 0.71073$ Å) radiation using the $\omega/2\theta$ scan mode at 24 °C in the range $2.07° \leq \theta \leq 26.00°$. An empirical absorption correction based on ψ scans was applied. Data were corrected with Lorentz and polarization effects during data reduction using XSCANS.[19] The structure was solved by direct methods and refined using SHELXTL 97 software.[20] All non-hydrogen atoms were refined anisotropically by full-matrix least squares techniques.

Hydrogen atoms for the carbon atoms were placed in their calculated positions with C–H = 0.96 Å, assigned fixed isotropic thermal parameters (1.2 times the atom to which they are attached), and allowed to ride on their respective parent atoms. The relevant crystal data and structural parameters are summarized in Table 1.

CCDC reference number 156015.

See http://www.rsc.org/suppdata/dt/b1/b100159k/ for crystallographic data in CIF or other electronic format.

Physical measurements

Elemental analysis was performed on a Perkin-Elmer 240C. ES-MS were obtained from a Finnigan MAT LCQ ES Mass spectrometer with a mass to charge (m/z) range of 2000.

Table 1 Crystallographic data for [CuL(Cl)](ClO$_4$)

Formula	$C_6H_{17}Cl_2CuN_3O_5$
Formula weight	345.66
Crystal system	Monoclinic
Space group	$P2(1)/c$
T/K	297(2)
λ/Å	0.71073
Color of crystal, habit	Blue, prism
a/Å	10.330(2)
b/Å	11.6090(10)
c/Å	11.310(2)
β/°	107.540(10)
V/Å^3	1293.2(4)
Z	4
ρ_{calc}/g cm^{-3}	1.775
μ/mm^{-1}	2.115
Crystal size/mm	0.44 × 0.40 × 0.36
θ range/°	2.07 to 26.00
Reflections collected	2540
Independent reflections	2144 ($R_{int} = 0.0259$)
Max. and min. transmission	0.5346 and 0.4690
Data/restraints/parameters	2540/1/159
GOF on F^2	1.035
$R1$[a] [$I > 2\sigma(I)$]	0.0259
$WR2$ [$I > 2\sigma(I)$]	0.0651[b]

[a] $R1 = \Sigma||F_o| - |F_c||/\Sigma|F_o|$, $wR2 = [\Sigma w(|F_o|^2 - |F_c|^2)]/\Sigma|w(F_o)^2|^{1/2}$. [b] $w = 1/[(F_o^2)^2 + (0.0651P)^2 + 0.1118P]$, where $P = (F_o^2 + 2F_c^2)/3$.

Theoretical analysis

Ab initio study on I, its deprotonation mode and the nucleophilic ability of the Cu(II) alkoxide and the Cu(II) hydroxide were conducted at the Hartree–Fock level.[16,21] A minimal basis set STO-3G[22] was used to optimize the structure of CuL(H_2O), $CuH_{-1}L(H_2O)$ and CuL(OH) and a bigger basis set 3-21G*[23] was employed to perform a single point energy calculation. To achieve convergence, cut-offs on forces and step size were tightened and a quadratically convergent SCF procedure[24] was used, in which linear searches are involved when far from convergence and Newton–Raphson steps when close (unless the energy goes up). The crystal structure of the CuL complex was used as the initial geometry for optimization. The theoretical study was conducted using the Gaussian 94 package.[25]

Results and discussion

Cu(II) complexation constants for L

The Cu(II) complexation constants of the polyamine L were determined by potentiometric titration. Protonation constants of the ligand L have been reported in our previous paper.[14] When equimolar Cu(II) was added to the solution, the titration curve revealed a very long pH buffering range between pH 5.5 and 9 ($a = 1.0$ to 4.5), as shown in Fig. 1, which implies the formation of CuL and $CuH_{-1}L$. Three complex species, CuL, $CuH_{-1}L$ and $CuH_{-1}L(OH)$ are believed to exist in aqueous solution, as deduced from ES-MS experiments and theoretical analysis. Attempts to employ the dimer $Cu_2(H_{-1}L)_2$ failed because the concentration was too low (less than 1 ppm).

The complexation constants for L with Cu(II) *i.e.* K(CuL) and K_a are defined as follows:

$$L + Cu^{2+} \rightleftharpoons CuL \quad K(CuL) = [CuL]/[L][Cu^{2+}] \quad (1)$$

$$CuL \rightleftharpoons CuH_{-1}L + H^+ \quad K_{a1} = [CuH_{-1}L]a_{H^+}/[CuL] \quad (2)$$

$$CuH_{-1}L \rightleftharpoons CuH_{-1}L(OH) + H^+ \quad K_{a2} = [CuH_{-1}L(OH)]a_{H^+}/[CuH_{-1}L] \quad (3)$$

Here we ascribe the first deprotonation site to the coordinated alcoholic group, contrary to the cases in V, VI and VII,[15] in which the coordinated water at the equatorial position

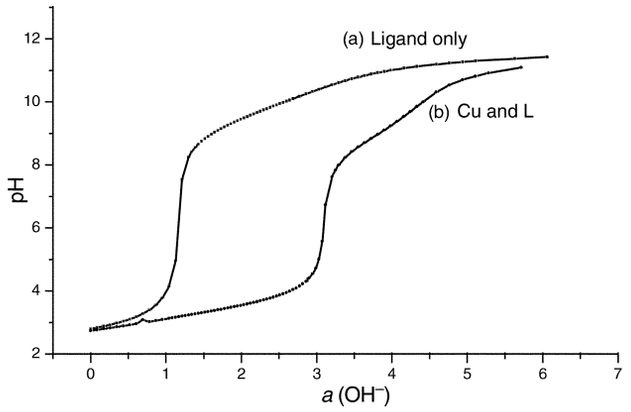

Fig. 1 Typical titration curve for L·3HCl at 25 °C and $I = 0.1$ M (NaCl). (a) 1.0 mM L·3HCl, σ fit *ca.* 0.03 after optimization by BEST; (b) 1.0 mM L·3HCl + 1.0 mM $CuSO_4$, σ fit *ca.* 0.04 after optimization by BEST.

is believed to be more acidic due to the shorter water oxygen–copper bond length. The ES-MS spectra gave implicit evidence for the presence of the Cu(II) alkoxide in aqueous solution, which is discussed in detail below. With the coordination of Cu(II), the deprotonation constant of the alcoholic OH group is significantly lowered to 8.5, whilst the basicity of the coordinated H_2O ($pK_{a2} = 10.6$, Scheme 2) is increased. This compares favourably with the stepwise deprotonation in [ZnL(H_2O)], II [14] and [Zn(phenol-pendant [12]aneN$_3$)(H_2O)].[26,27] The association constant of log K(CuL) at 25 °C is calculated to be 15.68 ± 0.06.

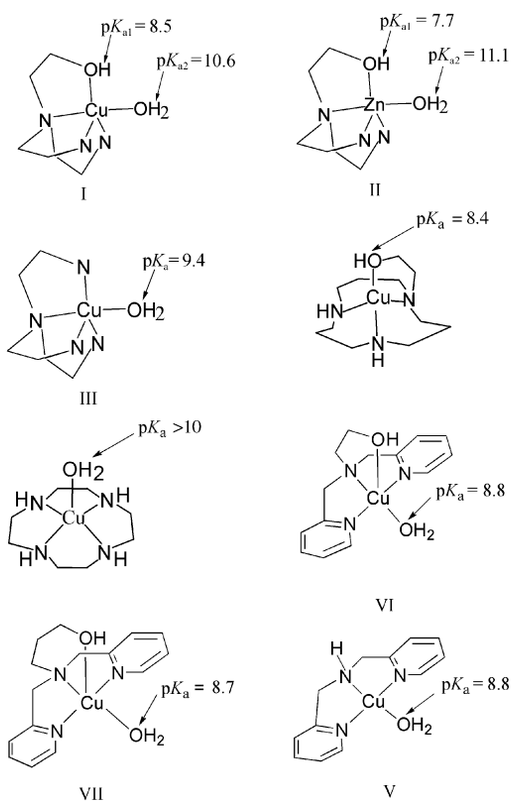

Scheme 2

Electrospray mass spectroscopy (ES-MS) data obtained for the present complex at pH 7.7 indicate the formation of 1 : 1 complexes: $[CuH_{-1}L]^+$ (*m*/*z* 209), $[CuH_{-1}L(CH_3OH)]^+$ (*m*/*z* 241) and $[CuL(CH_3CO_2)]^+$ (*m*/*z* 269) in aqueous solution, with no peaks corresponding to $[CuL(OH)]^+$ and $[Cu_2(H_{-1}L)_2]^{2+}$ being found. The peaks at *m*/*z* = 245 cause ambiguity

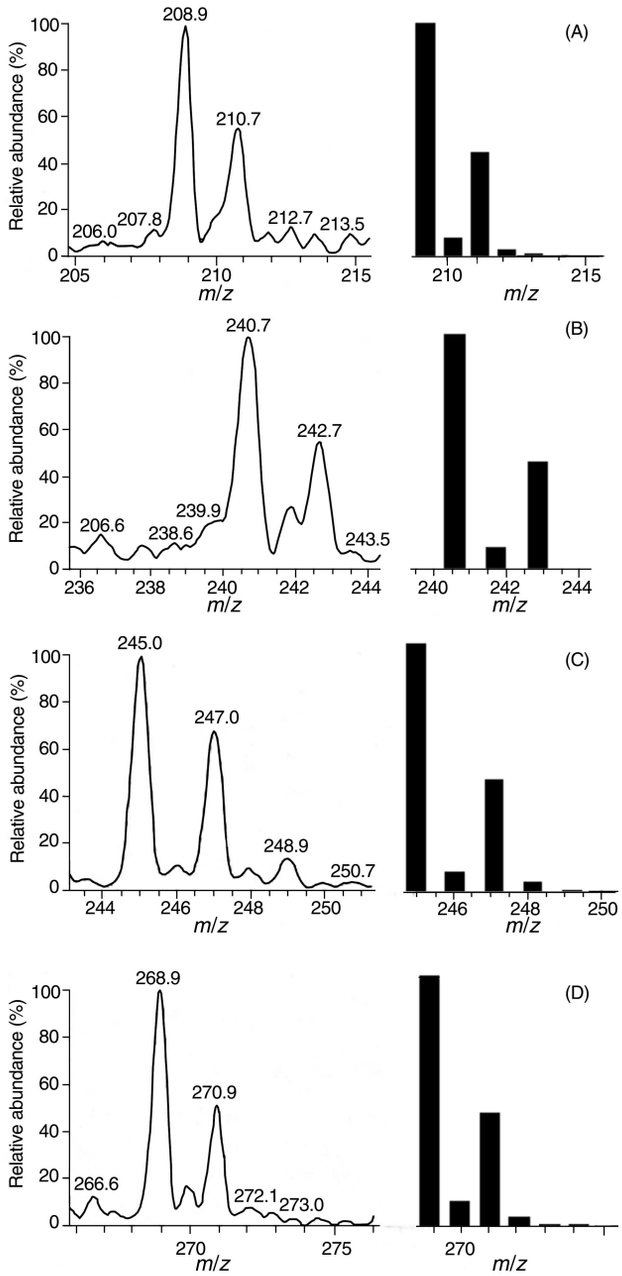

Fig. 2 ES-MS spectra of observed and calculated patterns for (A) $[CuH_{-1}L]^+$ (*m*/*z* 209), (B) $[CuH_{-1}L(CH_3OH)]^+$ (*m*/*z* 241), (C) $[CuH_{-1}L(OH_2)_2]^+$/$[CuL(OH)(OH_2)]^+$ (*m*/*z* 245) and (D) $[CuL(CH_3CO_2)]^+$ (*m*/*z* 269).

in assignment. Since the two species $[CuH_{-1}L(OH_2)_2]^+$ and $[CuL(OH)(OH_2)]^+$ have the same mass to charge ratio, ES-MS failed to distinguish them. Nevertheless, due to the rather significant occupancy values of $[CuH_{-1}L]^+$ and $[CuH_{-1}L(CH_3OH)]^+$ (sums up to *ca.* 30%) and the absence of the water-deprotonated species $[CuL(OH)]^+$, the Cu(II) alkoxide species are believed to be the major mono-deprotonated species present in the water–methanol solution at alkaline pH. Comparisons of the calculated and observed electrospray MS of selected peaks in the cation region are presented in Fig. 2.

A typical diagram for species distribution as a function of pH at [total Cu(II)] = [total L] = 1 mM, and 25 °C, is displayed in Fig. 3. It is found that CuL has the maximum occupancy of 99.8% at pH = 5.2, which is consistent with the strong coordination ability of the ligand L to Cu(II). In the weakly alkaline range, $CuH_{-1}L$ soon reaches the highest occupancy of 85.3% at pH 9.5, compared with the previous report for the

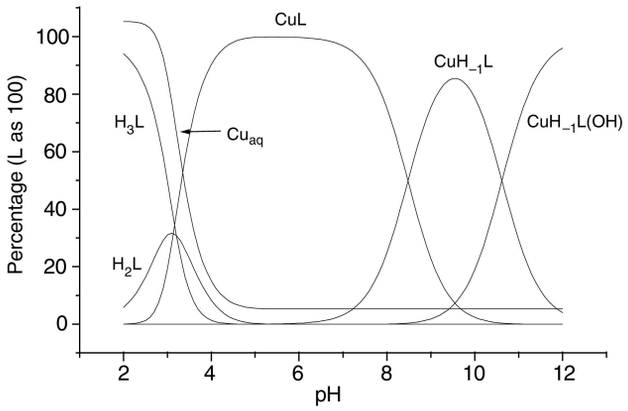

Fig. 3 Species distribution graph as a function of pH for the 1 mM L + 1 mM Cu(II) system at 25 °C and $I = 0.1$ M (NaCl).

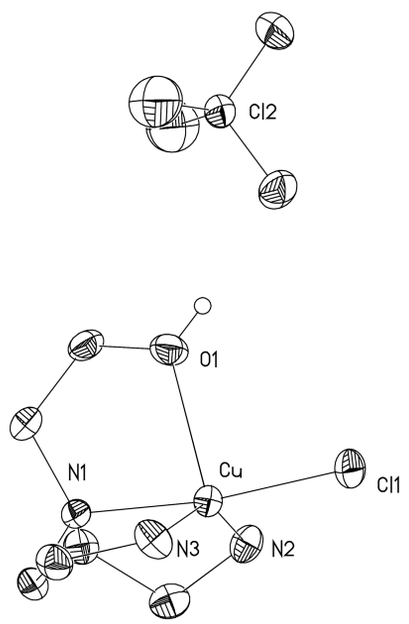

Fig. 4 An ORTEP[30] drawing (30% probability ellipsoids) of [CuL(Cl)](ClO_4). All hydrogen atoms bonded to carbon and nitrogen are omitted for clarity. The open circle attached to the oxygen atom represents the hydrogen atom, H1o.

ZnL complex: for $ZnH_{-1}L$, 91.5% at pH 9.4.[14] In strongly alkaline solution (pH > 11), the deprotonated and hydroxide-coordinated species $CuH_{-1}L(OH)$ becomes the major Cu(II)-containing species.

Single-crystal X-ray structure of [CuL(Cl)](ClO_4)

As illustrated in Fig. 4, the Cu(II) atom is located in a distorted trigonal-bipyramidal environment formed by the four coordinating atoms (N_3O of the tripod) and a chloride ion. The Cu(II) atom lies 0.230 Å above the trigonal equatorial plane formed by the terminal N and O atoms of the tripod with N3–Cu–N2 = 145.2°, N2–Cu–O1 = 103.4° and N3–Cu–O1 = 107.1°, while the two axial sites are occupied by the apical N1 atom of the tripod and the Cl with a N1–Cu–Cl1 angle of 172.9°. The distortion (Δ) of the coordination polyhedron from a regular trigonal bipyramid (TBP) ($\Delta = 0$) to the tetragonal pyramid ($\Delta = 1$) has been calculated according to the method reported by Anderegg and Muetterties.[28,29] The value of 0.35 indicates that the coordination geometry around Cu(II) is much closer to TBP. The Cu–O(alcohol) bond length, 2.286 Å, is longer than the previously reported M–O(alcohol) distance of 2.015 Å in the ZnL complex, and the average distance of 1.950 Å in the dimeric alcohol-pendant [12]aneN_3Zn(II) complex.[12] However, there are significant differences between the structures of the present Cu–tripodal polyamine complex and the previously reported [CuL'(Cl)]Cl·$3H_2O$ [L' = *N*-(2-hydroxyethyl)bis(2-benzimidazolylmethyl)amine],[15] in which the Cu(II) adopts square pyramidal coordination geometry with the alcoholic OH group in the apical position. This geometry is probably due to the rigidity of the benzimidazole group. In this square pyramidal complex, the equatorial Cu(II)–Cl bond (2.235 Å) is significantly shorter than the apical Cu(II)–O(ROH) bond (2.509 Å).[15] Since shorter water oxygen–copper bonds always lead to greater acidity and hence lower pK_a values,[15] the discrepancy in structure between [CuL(Cl)](ClO_4) and the previously reported N_3OX–copper complex may be responsible for the different deprotonation mode. Selected bond distances and angles for [CuL(Cl)](ClO_4) are given in Table 2.

Table 2 Selected bond distances (Å) and angles (°) for [CuL(Cl)](ClO_4)

Cu–O1	2.2861(19)	Cu–Cl1	2.2611(7)
Cu–N1	2.0432(18)	Cu–N2	2.0162(19)
Cu–N3	1.9952(19)		
N3–Cu–N2	145.22(9)	N3–Cu–N1	85.05(8)
N2–Cu–N1	84.81(8)	N3–Cu–Cl1	95.34(6)
N2–Cu–Cl1	98.67(6)	N1–Cu–Cl1	172.94(5)
N3–Cu–O1	107.12(9)	N2–Cu–O1	103.36(8)
N1–Cu–O1	78.80(7)	Cl1–Cu–O1	94.38(5)

Two kinds of hydrogen bonds occur in the structure. The strongest one, *i.e.* the hydrogen bond between O1 of the ethoxy-podand ligand and O2 of the perchlorate anion (O1 ··· O2 = 2.808 Å and O1–H1o ··· O2 = 169°), accompanied by the weak interaction between Cu(II) and the O atom of the adjacent perchlorate (bond distance being 3.424 Å) is responsible for the formation of the one-dimensional zigzag polymers which spread along the *a* axis to form infinite chains. The other kind of hydrogen bond exists among the chains between the primary amino groups of the ligand and the chlorine atoms: N2–H2a ··· Cl1 (x, $0.5 - y$, $0.5 + z$), N2 ··· Cl1 = 3.431 Å and N2–H2a ··· Cl1 = 153.26°, which cross-links the 1-D chains into one three-dimensional framework, as depicted in Fig. 5. The structure of the perchlorate anion is normal: the Cl–O bonds range from 1.397 Å to 1.428 Å while the angles of O–Cl–O are in the range from 109.6° to 111.51°.

CuL-promoted hydrolysis of 4-nitrophenyl acetate (NA)

The activity of the CuL complex in the promotion of carboxyester hydrolysis was tested. Since the phosphomonoesters underwent extremely slow hydrolysis with CuL similar to other N_3O–M(II) complexes (M = Zn or Cu, II to VII), the carboxyester 4-nitrophenyl acetate (NA) was used as a substitute.[11,12,14,31] The hydrolysis of NA (0.5–1.0 mM) promoted by CuL with concentrations varying from 0.4 mM to 2.0 mM at $I = 0.10$ M (90 mM $NaNO_3$) and pH 8.1, 8.5 and 8.9 (20 mM Tris·HCl buffers) in 10% (v/v) aqueous CH_3CN solution at 25#°C was followed by measuring the absorbance of released 4-nitrophenolate (NP) at 400 nm. The initial slope method was applied to the data processing procedure, as previously described in the literature.[11,12,14,31]

To elucidate the mechanism of the present CuL-promoted NA hydrolysis, we measured hydrolysis velocities both at constant NA concentration with varying total Cu(II) complex concentration and constant [total Cu(II) complex] with varied [NA]. The blank hydrolytic process without CuL as promoter was studied at the corresponding pH; this gave the spontaneous hydrolysis constant, known as v_{buffer}. Initial velocities (v_{total}) were measured by following the absorbance increases up to 5% of the extent of reaction. Since the concentrations of both the substrate NA and promoter CuL were essentially kept constant during the measurement, the absorbance increases

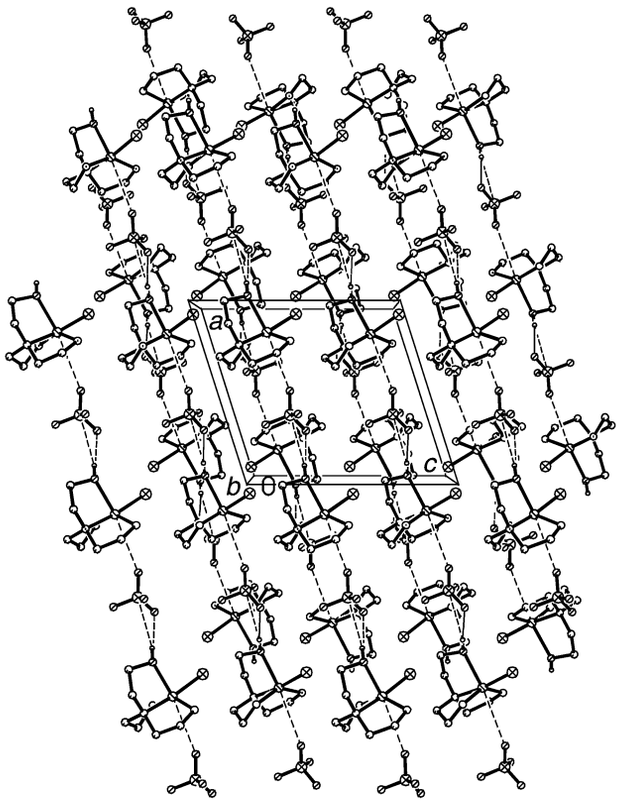

Fig. 5 Packing diagram viewed down the *b*-axis, showing the arrangement of the zigzag chains.

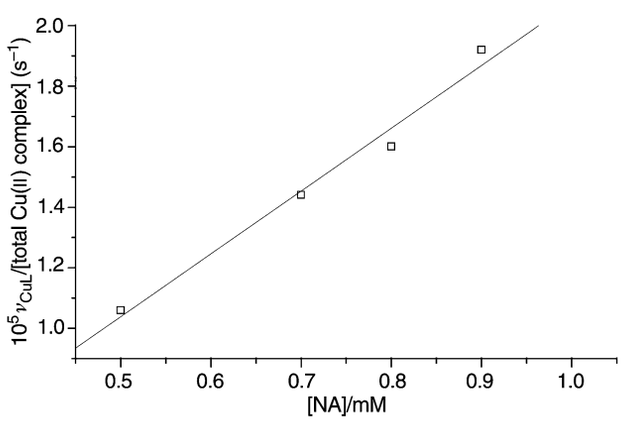

Fig. 6 Dependence of v_{CuL}/[total Cu(II) complex] on [NA] at pH 8.5 and constant [total Cu(II) complex], ionic strength 0.1 M, and at 25 °C in the presence of 10% (v/v) CH_3CN. The slope of the line gives k_{obs}. Correlation coefficient 0.991, observed rate corrected for spontaneous hydrolysis.

linearly (correlation coefficient >0.99) with the slope being v_{total}. The value of v_{CuL} was obtained by eliminating the effect of the buffer as ($v_{total} - v_{buffer}$). When [total Cu(II) complex] was set to be constant, the observed rate constant k_{obs} was calculated from the slope of the straight line v_{CuL}/[total Cu(II) complex] *vs.* [NA], see Fig. 6. This indicates that the rate is first-order with respect to the substrate. On the other hand, at the same pH, when [NA] was set to be constant, k_{obs} was also measured in the presence of various concentrations of CuL (0.4–2.0 mM).[31] The plot of v_{CuL}/[NA] *vs.* [total Cu(II) complexes] gave another straight line with the slope denoted as k_{obs}, an example of which is illustrated in Fig. 7, which testifies that the rate is also first-order with respect to the promoter. The two data processing strategies gave the same k_{obs}, 0.023 ± 0.002 M^{-1} s^{-1} at pH 8.5.

Hence, we conclude that the CuL-promoted hydrolysis is first-order with respect to both the CuL complex and NA ester,

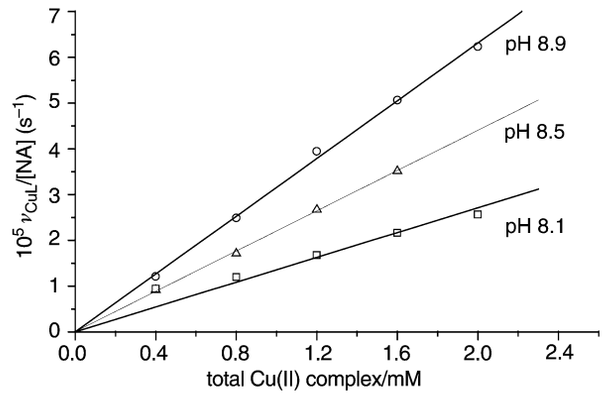

Fig. 7 Dependence of v_{CuL}/[NA] on [total Cu(II) complex] at pH 8.1, 8.5 and 8.9 and constant [NA], ionic strength 0.1 M, and at 25 °C in the presence of 10% (v/v) CH_3CN. The slope gives k_{obs}. Correlation coefficient >0.99, observed rate corrected for spontaneous hydrolysis.

Table 3 A comparison of hydrolysis rate constants, k_{NA} (M^{-1} s^{-1}) for CuL and other complexes, and aqueous OH^- ion at $I = 0.1$ M ($NaNO_3$) and 25 °C in 10% (v/v) CH_3CN

Promoter[e]	k_{NA}	Promoter[e]	k_{NA}
I	0.043 ± 0.002	II	0.13[a]
III	0.14[b]	IV	0.46[c]
[Cu(dipy)$(H_2O)_2$]	0.16[d]	OH^-_{aq}	8.1[b]

[a] From ref. 14. [b] From ref. 12. [c] From ref. 11. [d] From ref. 32. [e] The actual nucleophiles are $ZnH_{-1}L$ for II, III and IV and $CuH_{-1}L$ for I.

which is consistent with that previously reported for the Zn(II) complex hydrolytic cleavage of carboxyl esters. The initial rate constant k_{in}, observed rate constant k_{obs} and second-order rate constant k_{NA} are defined as follows:

$$v_{total} = v_{CuL} + v_{buffer} = k_{in}[NA]$$
$$v_{CuL} = k_{obs}[\text{total Cu(II) complex}][NA] = k_{NA}[CuH_{-1}L][NA]$$
$$v_{buffer} = (k_{OH^-}[OH^-] + ...)[NA]$$

The observed rate constants k_{obs} (all at 25 °C) are 0.032 ± 0.002 M^{-1} s^{-1} at pH 8.9, 0.023 ± 0.002 M^{-1} s^{-1} at pH 8.5 and 0.010 ± 0.002 M^{-1} s^{-1} at pH 8.1, which is proportional to the concentration of $CuH_{-1}L$.

The second-order rate constant k_{NA} for $CuH_{-1}L$ of 0.043 ± 0.002 M^{-1} s^{-1}, calculated from k_{obs} with the aid of the species distribution diagram (see Fig. 3), is compared with some k_{NA} values for NA hydrolysis promoted by other copper and zinc complexes in Table 3.

Mechanism

As has been suggested by Kimura[7] and Chin,[15] the metal alkoxide promoted hydrolysis involves the generation of covalent intermediates which have been separated and characterized by NMR spectroscopy as well as by HPLC and MS. Our attempts to separate the covalent intermediates (here, it is believed to be the product) were not successful. To examine whether the whole process is a hydrolysis or a transesterification, we followed the release of NP up to more than one cycle with the NA concentration set at 3 mM and with a CuL concentration of only 0.1 mM at *ca* 25 °C (to ensure the pseudo first-order environment with respect to the substrate, NA). The resulting v_{total} *vs.* time curve revealed that the mechanism was a transesterification instead of a hydrolysis. In the first period of reaction, *i.e.* where the CuL and buffer both catalyze the cleavage of NA, the velocity reduces in a time dependent manner, indicating that CuL is being consumed; however 8 minutes later the velocity becomes time-independent since the

Table 4 Results of the theoretical analysis on the *ab initio* Hartree–Fock level. All complexes are optimized at the STO-3G level and analyzed at the 3-21G* level

	$CuL(H_2O)$	CuL(OH)	$CuH_{-1}L(H_2O)$
Charge on the Cu(II)	1.175895	1.052778	1.073545
Charge on alcoholic O[a]	−0.753810 (−0.294946)	−0.690115(−0.240492)	−0.861293(−0.861293)
Charge on the water O[a]	−0.743850 (0.183913)	−0.893781(−0.538305)	−0.759437(0.166558)
HOMO[b]	−1.39555	−0.99867	−0.92481
HF Energy on 3-21G*	−2178.9407285	−2178.6074296	−2178.6286746

[a] The figures listed are the overall charge distribution on the oxygen atom only; the figures in parentheses are the charge with hydrogens summed into heavy atoms. [b] The HOMO of the $CuL(H_2O)$, *i.e.* I, does not reflect the character of the oxygen lone-pair electrons since the molecular orbital coefficients of oxygen atomic orbits are rather small; however, in the cases for Ia and Ib, the atomic orbitals of oxygen in active sites have the highest occupancy in the HOMO, hence the HOMO reflects the character of the oxygen lone-pair electrons.

buffer is then the sole promoter. The results indicate that the acyl-coordinated species is probably the final product, and the subsequent hydrolysis is hindered. This is different from the previously demonstrated double-hydrolysis cycle of NA catalyzed by Zn(II) complexes.

Herein, we suggest that CuL cleaves NA mainly through the metal alkoxide transesterification path. The proposed mechanism is depicted in Scheme 3. In conclusion, we have shown that a simple metal complex with both a pendant alcoholic group and one coordination site for external H_2O/HO^- can efficiently cleave the activated carboxyl ester, NA and the metal alkoxide promoted transesterification path is more preferable than the metal hydroxide promoted hydrolysis path. This evidence may relate to the role of metal alkoxides in hydrolytic enzymes such as alkaline phosphatase.

Ab initio analysis of the deprotonation mode and nucleophilic ability of the deprotonated species

To provide further evidence for the stronger acidity of the Cu-bound alcohol over the Cu-bound water and the stronger nucleophilic ability of the Cu–alkoxide over Cu–hydroxide, we conducted an *ab initio* Hartree–Fock type analysis.[16] The dissociation energy of H_2O into H^+ and OH^- was also calculated to assess the accuracy of the previously described method, the experimental and calculated values are 1720 kJ mol^{-1} and 1745 kJ mol^{-1} respectively. All the results have been included in Table 4. Cu(II)-bound alkoxide is more favorable than Cu(II)-bound hydroxide, with the reaction energy difference, ΔE, 55.77 kJ mol^{-1} lower, indicating the preference for formation of the alkoxide species. From these facts we can safely conclude that the first deprotonated site should be Cu(II)-coordinated alcohol instead of Cu(II)-coordinated water. The overall charge on the deprotonated RO^-/HO^- and energies of the HOMO having oxygen lone-pair character will give an indication of the order of nucleophilic ability. As illustrated in Table 4, both the oxygen atoms of the deprotonated RO^- in $CuH_{-1}L(H_2O)$ and of HO^- in CuL(OH) bear significant negative charge (−0.86 e and −0.89 e), indicating the location of the active site for ester cleavage. Though the HO^- in CuL(OH) is *ca.* 0.03 e more negative than the counterpart in $CuH_{-1}L(H_2O)$, the two adjacent $H^{\delta+}$ (one belongs to the alkoxide, +0.45 e; the other belongs to the hydroxide, +0.36 e) will strongly repel the substrate, which may encumber the interaction of the complex and the substrate. HOMO oxygen lone-pair energy for Cu(II) alkoxide is 0.148 eV higher than that of Cu(II) hydroxide, which implies that the nucleophile is more inclined to react with the electrophile having LUMO as acceptor, hence the nucleophilicity of the oxygen in Cu(II) alkoxide species is expected to be better. All the present results generated from *ab initio* analysis provide rather efficient evidence for the preference of the metal-bound alkoxide in the ester cleavage process.

Conclusion

A solution complexation study by potentiometric titration on the new Cu(II) complexes of tripodal ligand 2-[bis(2-aminoethyl)amino]ethanol L has revealed that when coordinated to Cu(II), the hydroxyl group of L deprotonates with a low pK_a value of 8.5, and then the coordinated water releases the second hydrogen atom with $pK_a = 10.6$ at 25 °C. Single-crystal X-ray diffraction analysis of $[CuLCl](ClO_4)$ revealed that Cu(II) adopts a trigonal-bipyramidal geometry, which is different from the previously reported N_3OX–copper complex. ES-MS analysis of an aqueous solution of the complex provided evidence for the existence of Cu(II) alkoxide. The CuL-promoted cleavage of 4-nitrophenyl acetate (NA) showed a second-order rate constant of 0.043 M^{-1} s^{-1}. The preference for the Cu(II) alkoxide promoted transesterification over Cu(II) hydroxide hydrolysis was demonstrated by kinetic experiments showing evidence for the stronger nucleophilic ability of the metal alkoxide compared to the metal hydroxide. Additionally, *ab initio* Hartree–Fock studies strongly suggest that the Cu(II) alkoxide will be generated prior to Cu(II) hydroxide due energetic preferences,

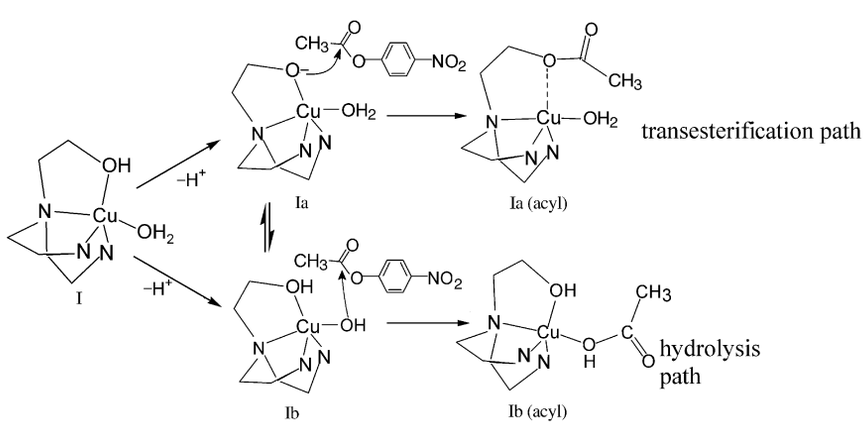

Scheme 3

i.e. the Cu(II) coordinated alcohol will exhibit a lower pK_a than Cu(II) coordinated water. Though charge distribution on the oxygen atom of Cu(II) hydroxide is somewhat more negative than the Cu(II) alkoxide, when the effect of the adjacent hydrogen atoms is taken into consideration, the latter will exhibit greater nucleophilic ability. Mulliken population analysis showed that the HOMO oxygen lone-pair energy for Cu(II) alkoxide is 0.148 eV higher than that of Cu(II) hydroxide, and accordingly the nucleophilicity of the oxygen of Cu(II) alkoxide is expected to be greater.

Acknowledgements

This work is supported by the National Natural Science Foundation of China. We are indebted to Professor Miao Qiang for helpful discussions and sincere assistance. We would like to express our gratitude to the referees for their useful and detailed suggestions.

References

1 B.L. Vallee and D.S. Auld, *Acc. Chem. Res.*, 1993, **26**, 543.
2 J. Chin, *Acc. Chem. Res.*, 1991, **24**, 145.
3 N. H. Williams, B. Takasaki, M. Wall and J. Chin, *Acc. Chem. Res.*, 1999, **32**, 485.
4 W. N. Lipscome and N. Strater, *Chem. Rev.*, 1996, **96**, 2396.
5 P. Molenveld, J. F. J. Engbersen and D. Reinhoudt, *Chem. Soc. Rev.*, 2000, **29**, 75.
6 J. Chin, S. S. Lee, K. J. Lee, S. Park and D. H. Kim, *Nature (London)*, 1999, **401**, 254.
7 E. Kimura and E. Kikuta, *J. Biol. Inorg. Chem.*, 2000, **5**, 139.
8 E. E. Kim and H. W. Wyckoff, *J. Mol. Biol.*, 1991, **218**, 449.
9 J. E. Coleman, *Annu. Rev. Biophys. Biomol. Struct.*, 1992, **21**, 441.
10 T. A. Steitz and J. A. Steitz, *Proc. Natl. Acad. Sci. U. S. A.*, 1993, **90**, 6498.
11 T. Koike, S. Kajitani, I. Nakamura, E. Kimura and M. Shiro, *J. Am. Chem. Soc.*, 1995, **117**, 1210.
12 E. Kimura, I. Nakamura, T. Koike, M. Shionoya, Y. Kodama, T. Ikeda and M. Shiro, *J. Am. Chem. Soc.*, 1994, **116**, 4764.
13 (*a*) I. O. Kady, B. Tan, Z. Ho and T. Scarborough, *J. Chem. Soc., Chem. Commun.*, 1995, 1137; (*b*) D. S. Sigman and C. T. Jorgensen, *J. Am. Chem. Soc.*, 1972, **94**, 1724; (*c*) S. H. Gellman, R. Petter and R. Breslow, *J. Am. Chem. Soc.*, 1986, **108**, 2388; (*d*) J. G. Weijnen, A. Koudijs and J. F. Engbersen, *J. Org. Chem.*, 1992, **57**, 7258; (*e*) M. A. De Rosch and M. C. Trogler, *Inorg. Chem.*, 1990, **29**, 2409.
14 J. Xia, Y. Xu, S. A. Li, K. B. Yu and W. X. Tang, *Inorg. Chem.*, 2001, **40**, 2394.
15 M. J. Young, D. Wahnon, R. C. Hynes and J. Chin, *J. Am. Chem. Soc.*, 1995, **117**, 9441.
16 I. Bertini, C. Luchinat, M. Rosi, A. Sgamellotti and F. Tarantelli, *Inorg. Chem.*, 1990, **29**, 1460.
17 V. A. Bobylev and V. D. Chechik, *Zh. Obshch. Khim.*, 1990, **60**, 2721.
18 A. E. Martell and R. J. Motekaitis, in *Determination and Use of Stability Constants*, 2nd edn., VCH Publishers, Inc., New York, 1992.
19 XSCANS Version 2.1, Siemens Analytical X-Ray Instruments Inc., Madison, WI, 1994.
20 G. M. Sheldrick, SHELXTL 97, Program for Crystal Structure Determinations, University of Göttingen, 1997.
21 P. A. Kollman, *Acc. Chem. Res.*, 1996, **29**, 461.
22 (*a*) W. J. Hehre, R. F. Stewart and J. A. Pople, *J. Chem. Phys.*, 1969, **51**, 2657; (*b*) J. B. Collins, P. v. R. Schleyer, J. S. Binkley and J. A. Pople, *J. Chem. Phys.*, 1976, **64**, 5142.
23 (*a*) J. S. Binkley, J. A. Pople and W. J. Hehre, *J. Am. Chem. Soc.*, 1980, **102**, 939; (*b*) M. S. Gordon, J. S. Binkley, J. A. Pople, W. J. Pietro and W. J. Hehre, *J. Am. Chem. Soc.*, 1982, **104**, 2797; (*c*) W. J. Pietro, M. M. Francl, W. J. Hehre, D. J. Defrees, J. A. Pople and J. S. Binkley, *J. Am. Chem. Soc.*, 1982, **104**, 5039; (*d*) K. D. Dobbs and W.J. Hehre, *J. Comp. Chem.*, 1986, **7**, 359; (*e*) K. D. Dobbs and W. J. Hehre, *J. Comp. Chem.*, 1987, **8**, 861; (*f*) K. D. Dobbs and W. J. Hehre, *J. Comp. Chem.*, 1987, **9**, 880.
24 G. B. Bacskay, *Chem. Phys.*, 1981, **61**, 385.
25 M. J. Frisch, G. W. Trucks, H. B. Schlegel, P. M. W. Gill, B. G. Johnson, M. A. Robb, J. R. Cheeseman, T. Keith, G. A. Petersson, J. A. Montgomery, K. Raghavachari, M. A. Al-Laham, V. G. Zakrzewski, J. V. Ortiz, J. B. Foresman, J. Cioslowski, B. B. Stefanov, A. Nanayakkara, M. Challacombe, C. Y. Peng, P. Y. Ayala, W. Chen, M. W. Wong, J. L. Andres, E. S. Replogle, R. Gomperts, R. L. Martin, D. J. Fox, J. S. Binkley, D. J. Defrees, J. Baker, J. P. Stewart, M. Head-Gordon, C. Gonzalez and J. A. Pople, Gaussian 94, Revision E.1, Gaussian, Inc., Pittsburgh, PA, 1995.
26 E. Kimura, M. Yamaoka, M. Morioka and T. Koike, *Inorg. Chem.*, 1986, **25**, 3883.
27 E. Kimura, T. Koike and K. Toriumi, *Inorg. Chem.*, 1988, **27**, 3687.
28 G. Anderegg and V. Gramlich, *Helv. Chim. Acta*, 1994, **77**, 685.
29 E. L. Muetterties and L. J. Guggenberger, *J. Am. Chem. Soc.*, 1974, **96**, 1748.
30 C. K. Johnson, ORTEP, Report ORNL-5138, Oak Ridge National Laboratory, Oak Ridge, TN, 1976.
31 J. Suh, S. J. Son and M. P. Suh, *Inorg. Chem.*, 1998, **37**, 4872.
32 J. Chin and V. J. Jubian, *J. Chem. Soc., Chem. Commun.*, 1989, 839.